 ©2021 Kvantovaya Elektronika and IOP Publishing Limited

https://doi.org/10.1070/QEL17474

In vivo non-invasive determination of the water concentration and water bonding properties in the human stratum corneum using confocal Raman microspectroscopy (mini-review)

M.E. Darvin, C.S. Choe, J. Schleusener, J. Lademann

Abstract. **Water plays an important role for normal functioning of the skin. The stratum corneum (SC) – the outermost layer of the epidermis – maintains the skin barrier function and regulates the water balance in the organism. Water is non-homogeneously distributed in the SC and its correct determination is important in dermatology and cosmetology. Confocal Raman microspectroscopy (CRM) is the most suitable non-invasive method to determine depth profiles of the water concentration, water with different mobility and hydrogen bonding states of water molecules in human skin *in vivo*, i.e. to study the SC hydration and moisturising. An *in vivo* application of CRM on normal human skin for investigation of the water concentration and water bonding properties in the SC is reviewed in this paper. Investigations performed on volunteers of two age groups reveal changes, which show that the SC of older skin binds water more efficiently compared to younger skin.**

Keywords: *skin barrier function, skin hydration, skin moisturising, water mobility, intercellular lipids, epidermis, ageing.*

1. Introduction

The stratum corneum (SC), the uppermost layer of the epidermis, consist of corneocytes embedded with intercellular lipids, which maintains the skin barrier function, i.e. provides protection against external physical and chemical influences, impedes the penetration of pathogens into the body and plays an important role in regulation of the water balance in the organism. The main components of the SC are keratin, lipids, natural moisturising factor (NMF) molecules and water. The SC also contains carotenoids and melanin. All SC components are non-homogeneously distributed throughout the SC depth [1, 2]. The water concentration is minimal in the superficial SC and maximal at the bottom of the SC [3]; the total water concentration in the SC varies between 0.20–0.78 g cm^{-3} [4]. Water is necessary for the SC, as it serves as a medium for numerous enzymes and other substances that make the SC metabolically active. The main centres of water binding in the SC are NMF molecules [5] and keratin [6] inside the corneocytes, and, to a lesser extent, the lamellar structure of extracellular lipids [7] between the corneocytes. The efficacy of water binding is nonuniform and depends on the SC depth [8, 9].

Water concentration in the skin is an important physiological parameter for controlling the hydration degree of dry and dehydrated skin, for diagnosing a number of skin diseases, and for the treatment control. The use of non-invasive *in vivo* methods is indispensable for this task. For non-invasive *in vivo* measurement of the water content in human skin, the electrical (corneometry) [10, 11], optical (IR spectroscopy [12, 13], reflection spectroscopy in the near-infrared range [14–16], confocal Raman microspectroscopy (CRM) [3, 17, 18]) and other methods [19–24] are used.

Electrical methods include measurements of electrical conductivity and capacitance of the skin. Conductance values correlate well with the water content in the superficial depth up to 15 μm, i.e. in the SC, while the capacitance values correlate with the water content in the depth up to 45 μm, i.e. in the papillary dermis [25, 26]. Thus, these methods can be used to determine SC dryness and dermal dehydration, respectively. The advantages of electrical methods (corneometry) are low costs of the devices and an easy measurement procedure. The disadvantages include the low measurement stability, which may depend additionally on external factors such as temperature and humidity, as well as skin surface moisture, influenced by sweating, transepidermal water loss (TEWL), the presence of cosmetics on the skin surface, and the quality of contact between the sensor and the skin surface during measurements. In addition, conductivity and capacitance measurements are carried out integrally and do not provide information about the water distribution gradient.

In the red and near-infrared optical range, the skin is characterised by low absorption and scattering coefficients (also termed 'spectral transparency window of the skin') [27] and by low fluorescence intensity [28], which determine the frequent selection of these wavelengths for skin measurements. Water absorption is strongly increased in the near-infrared range starting from ~1 μm [29, 30]. For this reason, reflection spectroscopy of water is mainly performed in this optical range [14, 16]. Optical laser-based microscopic methods operated in the red and near-infrared regions are very promising for non-invasive water measurements and, due to the availability of intensity stable lasers, are characterised by high measurement accuracy and the possibility to identify the

M.E. Darvin, J. Schleusener, J. Lademann Charité – Universitätsmedizin Berlin, corporate member of Freie Universität Berlin, Humboldt-Universität zu Berlin; Berlin Institute of Health, Department of Dermatology, Venerology and Allergology, Center of Experimental and Applied Cutaneous Physiology, Charitéplatz 1, 10117 Berlin, Germany; e-mail: maxim.darvin@charite.de;
C.S. Choe Kim Il Sung University, Ryongnam-Dong, Taesong District, Pyongyang, DPR Korea

Received 3 November 2020
Kvantovaya Elektronika **51** (1) 28–32 (2021)
Submitted in English

water distribution profile with micron resolution. An advantage of CRM is the possibility to perform non-invasive *in vivo* measurements of the water concentration [13, 31, 32] and the hydrogen bonding state of water molecules [18, 33], as well as distribution profiles from the SC towards the papillary dermis layer. In investigation of the SC, it was postulated that keratin, the main protein of the SC, can be used for normalisation of the depth dependent signal attenuation [34].

This mini-review represents the depth profiles of the water concentration, depending on its mobility state and the water bonding properties in the SC obtained *in vivo* on healthy human volunteers of two age groups using CRM. The CRM method is specified and the obtained results are discussed.

2. Materials and methods

Measurements were performed non-invasively and *in vivo* on the volar forearm skin of 11 healthy volunteers aged from 23 to 62 years using a confocal Raman microscope (Model 3510, RiverD International B.V., Rotterdam, The Netherlands). The fingerprint region (FP, 400–2000 cm^{-1}) was excited using a laser at 785 nm (exposure time 5 s, 20 mW); the high wavenumber region (HWN, 2000–4000 cm^{-1}) was excited using a laser at 671 nm (exposure time 1 s, 17 mW). The spatial resolution was less than 5 μm and the spectral resolution was less than 2 cm^{-1}. Raman spectra in the FP and HWN regions were recorded at the same position on the skin at 2 μm increments between the position of approximately 10 μm above the surface and 30 μm below the surface. The exact position of the skin surface was determined based on half the maximal keratin profile measured at ~1650 cm^{-1} [3] and the thickness of the SC was determined at the position, where the water concentration gradient reached 0.5, which is the border between the SC and the stratum granulosum [35]. Before processing the Raman spectra in the HWN region, the fluorescence background was removed using a piecewise-weighted-least squares fitting algorithm, described in [18].

A decomposition of the Raman bands in the HWN region was performed by a multiple nonlinear regression method using 10 Gaussian functions. Initial centre positions for the Gaussian functions were indicated at 2850 cm^{-1} (symmetric CH stretch vibrations of lipids), 2880 cm^{-1} (asymmetric CH stretch vibrations of lipids), 2930 cm^{-1} (symmetric CH_3 stretching vibrations of keratin), 2980 cm^{-1} (asymmetric CH_3 stretching vibrations of keratin), 3005 cm^{-1} (tightly bound water, DAA), 3060 cm^{-1} (olefinic CH stretching vibration of keratin), 3280 cm^{-1} (strongly bound water, DDAA), 3330 cm^{-1} (NH vibration of keratin), 3460 cm^{-1} (weakly bound, DA), and 3604 cm^{-1} ('free' water). All data analysis was performed in Matlab R2015a (The Mathworks, Inc., Natick, USA).

A positive vote for the measurements had been obtained from the Ethics Committee of the Charité–Universitätsmedizin Berlin and all procedures complied with the Declaration of Helsinki.

3. Results and discussion

Water is characterised by an intensive Raman spectrum in a broad wavenumber range of abour 3000–3700 cm^{-1} (valence vibrations of the OH group). Usually, the water concentration in the SC is calculated by the ratio between the water-related Raman band (3350–3550 cm^{-1} region) and the protein-related Raman band (2910–2965 cm^{-1} region) [3, 34]. The regions are schematically shown in Fig. 1a. In case of skin treated with cosmetic formulations, the normalisation by the Amide I Raman band at 1650 cm^{-1} is generally recommended due to the absence or controlled superposition on the 2910–2965 cm^{-1} region [36, 37]. Normalisation on a keratin-related Raman band is essential to take into account the depth-dependent signal attenuation (laser excitation and Raman signals) induced by absorption and diffuse scattering of the skin. As recently shown, the concentration of keratin decreases from the surface towards the bottom due to an increase in the water concentration, which can be considered by modelling the signal attenuation in the SC [38]. The results show that taking the inhomogeneity of the keratin concentration in the SC into account results in slightly decreased values for the water concentration at the

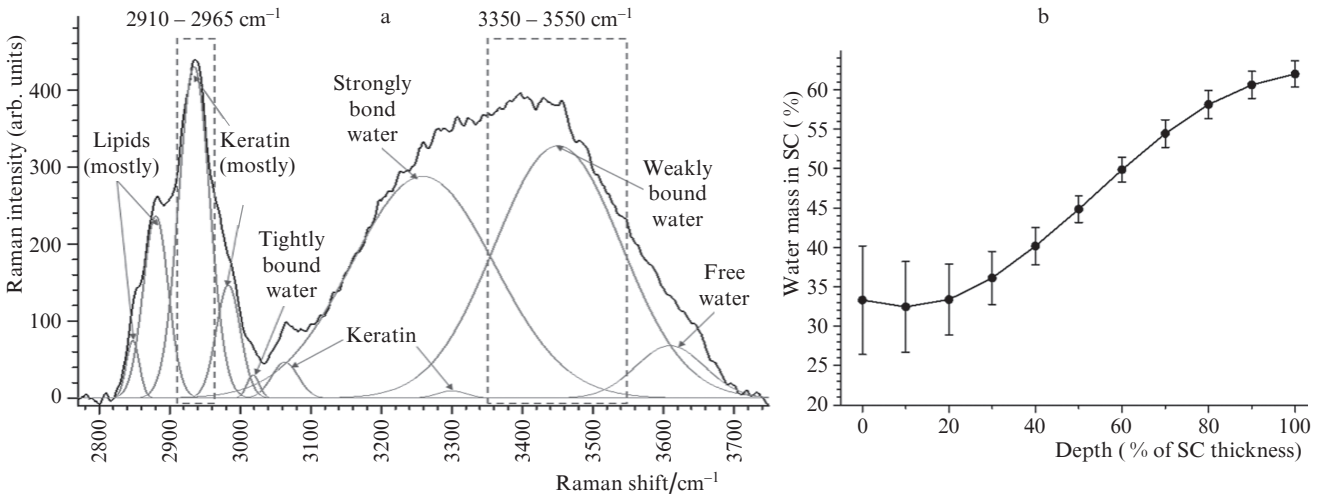

Figure 1. (a) Raman spectrum of the human volar forearm SC *in vivo* at 20 μm depth (SC thickness is 20 μm) in the 2780–3750 cm^{-1} region decomposed using Gaussian lines and (b) the depth profile of the water concentration obtained by the $I_{3350-3550}/I_{2910-2965}$ ratio taking the inhomogeneity of keratin distribution in the SC into account. Figures are adapted from [1, 18].

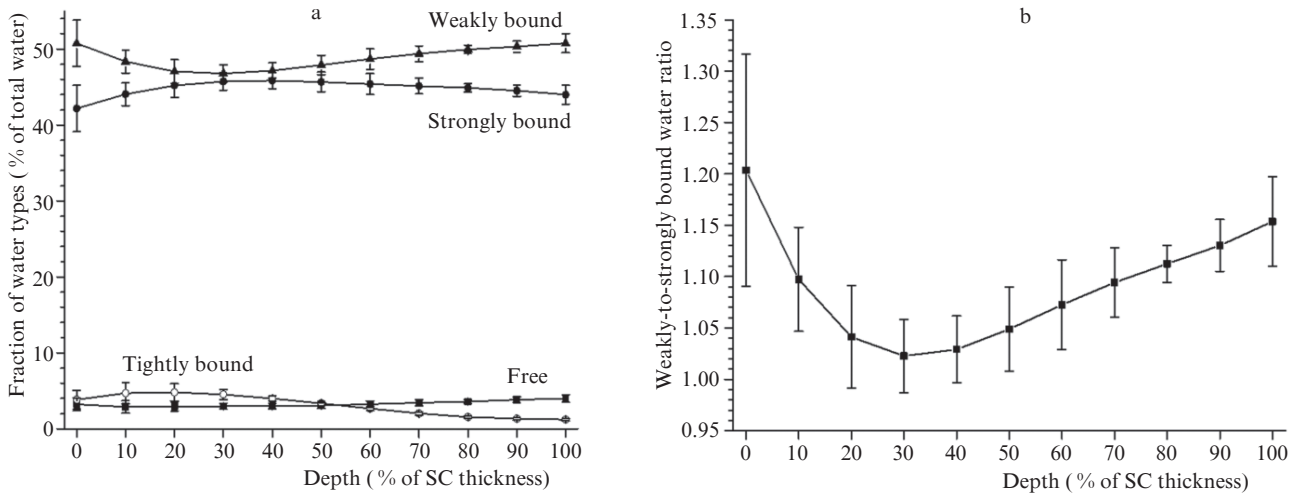

Figure 2. (a) Human SC depth profiles of the concentration of water molecules with different mobility depending on the strength of hydrogen bonds and (b) hydrogen bonding state of water measured *in vivo* using CRM. Figures are adapted from [18].

50%–100% SC depth ($p < 0.05$) [1]. The water concentration profile in the SC, calculated by taking the inhomogeneity of the keratin distribution in the SC into account is presented in Fig. 1b. The water concentration is non-homogeneous in the SC: the minimum concentration (~33%) is achieved in the superficial depth (0–20% SC depth). Further, the water concentration uniformly increases and reaches its maximum (~62%) at the boundary between the SC and stratum granulosum (100% SC depth).

The Raman spectrum of water in the ~3000–3750 cm^{-1} region contains information about the water mobility as follows: lower/higher wavenumbers correspond to highest/lowest hydrogen bonding strength of water with surrounding molecules, i.e. lowest/highest water mobility [39, 40]. A Gaussian function-based decomposition of the Raman spectrum of the human SC is presented in Fig. 1a, showing the superposition of the keratin-related Raman bands at ~3063 cm^{-1} and at ~3330 cm^{-1} on the water spectrum. The decomposed Raman spectrum describes the water molecules with different mobility, i.e. with different hydrogen bonding states: ~3005 cm^{-1}, tightly bound water; ~3277 cm^{-1}, strongly-bound water; ~3458 cm^{-1}, weakly-bound water; and ~3604 cm^{-1}, unbound water [18].

Tracking the intensity of the corresponding Gaussian functions provides information about the distribution of different water types depending on the strength of the hydrogen bonds in the SC, which are presented in Fig. 2a. As can be seen, strongly and weakly bound water types represent more than 90% of the total water in the SC. The remaining part (less than 10%) represents tightly bound and unbound water types. The weakly-to-strongly bound water ratio represents a hydrogen bonding state of water molecules in the SC, which is shown in Fig. 2b. This is an important physiological parameter, which shows the bonding efficacy of water molecules in different SC depths. A lower value describes a better efficacy to bind water with surrounding SC molecules, which is observed at 20%–40% SC depth.

Human skin undergoes changes with increasing age [41, 42], which has an influence on water bonding in the SC [43]. Volunteers of a 'younger group' (23–34, mean 29 year old) and an 'older group' (45–62, mean 50 year old) were recruited to take part in a pilot study using CRM. With 21 ± 2 μm, the SC thickness in the older group was modestly thicker than in the younger group, where it was 19 ± 1 μm on the volar forearm ($p < 0.1$) [44]. Figure 3 shows the obtained results for distributions of the water concentration as functions its mobility state and the water bonding properties in the SC.

The distribution of the weakly and strongly bound water in the SC shows significant differences ($p < 0.05$) between the younger and older groups at 10%–30% SC depths. The SC of the 'younger group' contains more weakly and less strongly bound water compared to the 'older group' (Figs 3a and 3b). No differences were found in the distribution of tightly bound and unbound water (Figs 3c and 3d). The hydrogen bonding state of water is significantly higher in the 10%–30% SC depth of the 'older group' (Fig. 3e) that means a more efficient water binding compared to the 'younger group' at these depths. Thus, an increase of age results in increasing the water binding at exemplary SC depths, which can be related to increase of NMF concentration and orthorhombic organisation of intercellular lipids at 10%–30% SC depths [44]. These results are in agreement with findings of slightly lower TEWL in aged skin, indicating increased barrier function [45, 46]. However, TEWL does not contain information about skin hydration. It should be taken into consideration that the water binding in the SC could be different to that presented in Fig. 3 for volunteers of age over 70 years old., as at this age the intrinsic ageing is better pronounced and manifested clinically [47].

In conclusion, it can be summarised that depth profiles of the water concentration, water with different mobility, as well as the hydrogen bonding state of water molecules can be successfully and non-invasively determined *in vivo* in the human SC.

Acknowledgements. The work of M.E.D., J.S. and J.L. was supported by the Foundation for Skin Physiology of the Donor Association for German Science and Humanities. C.S.C. was supported by the German Academic Exchange Service (DAAD) during his research stay at the Department of Dermatology, Charité – Universitätsmedizin Berlin.

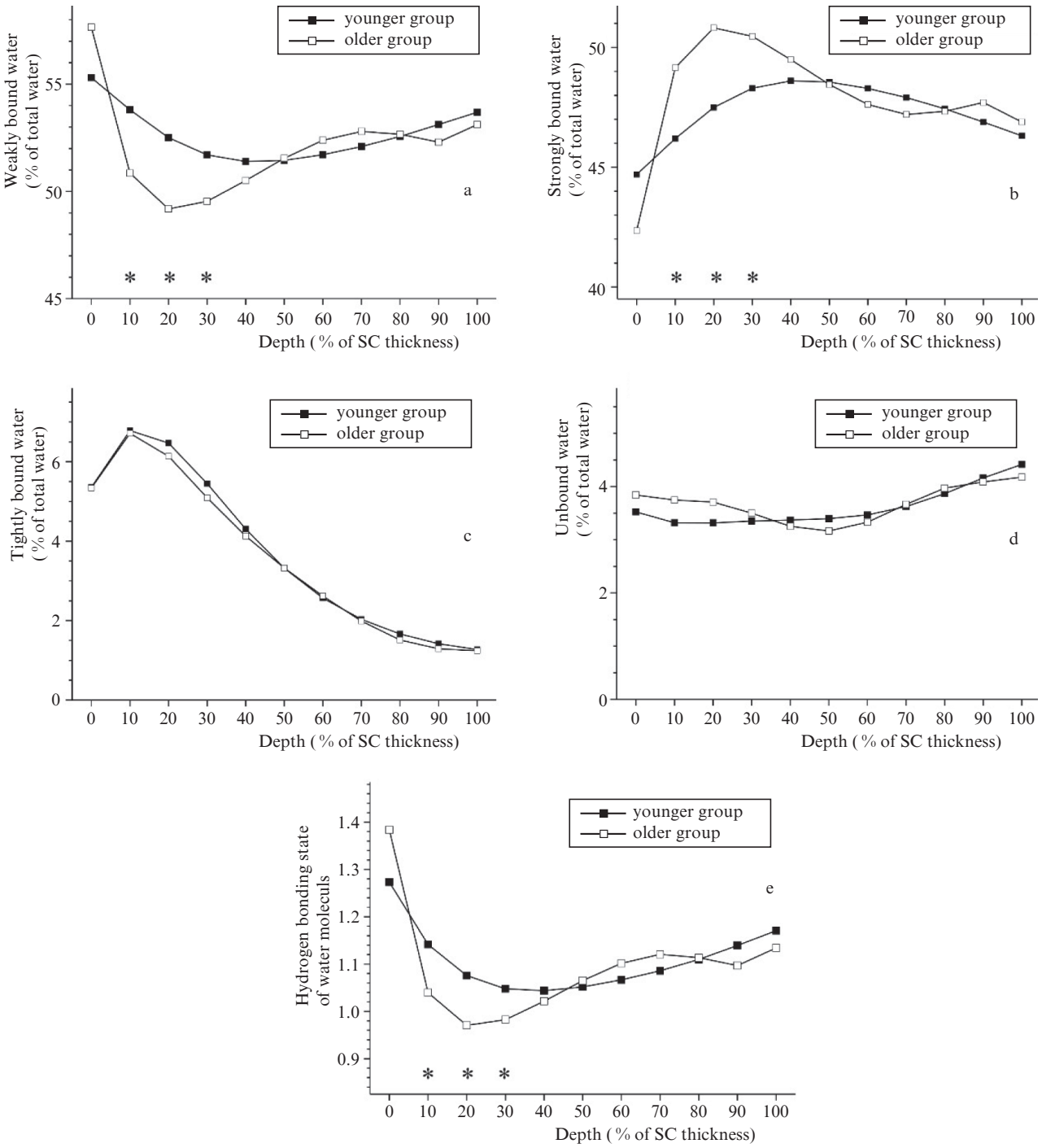

Figure 3. Depth profiles of (a) weakly bound, (b) strongly-bound, (c) tightly bound and (d) unbound water molecules and (e) the hydrogen bonding state of water in the SC of the 'younger group' (filled squares) and the 'older group' (empty squares) measured *in vivo* using CRM. The asterisk represents significant differences, $p < 0.05$. Figures are adapted from [44].

References

1. Darvin M.E., Choe C.S., Schleusener J., Lademann J. *Biomed. Opt. Express*, **10** (6), 3092 (2019).
2. Yakimov B.P., Shirshin E.A., Schleusener J., Allenova A.S., Fadeev V.V., Darvin M.E. *Sci. Rep.*, **20**, 14374 (2020).
3. Caspers P.J., Lucassen G.W., Bruining H.A., Puppels G.J. *J. Raman Spectrosc.*, **31** (8 – 9), 813 (2000).
4. Li X., Johnson R., Kasting G.B. *J. Pharm. Sci.*, **105** (3), 1141 (2016).
5. Rawlings A.V., Harding C.R. *Dermatol. Ther.*, **17** (1), 43 (2004).
6. Scheuplein R.J., Morgan L.J. *Nature*, **214** (5087), 456 (1967).
7. Imokawa G., Kuno H., Kawai M. *J. Investig. Dermatol.*, **96** (6), 845 (1991).
8. Choe C., Schleusener J., Lademann J., Darvin M.E. *Sci. Rep.*, **7** (1), 15900 (2017).
9. Caussin J., Groenink H.W., de Graaff A.M., Gooris G.S., Wiechers J.W., van Aelst A.C., Bouwstra J.A. *Exp. Dermatol.*, **16** (11), 891 (2007).
10. Tagami H. *Br. J. Dermatol.*, **171** (3), 29 (2014).
11. Utz S.R., Karakaeva A.V., Galkina E.M. *Saratov J. Med. Sci. Res.*, **10** (3), 512 (2014).
12. Potts R.O., Guzek D.B., Harris R.R., Mckie J.E. *Arch. Dermatol. Res.*, **277** (6), 489 (1985).

13. Lucassen G.W., van Veen G.N., Jansen J.A. *J. Biomed. Opt.*, **3** (3), 267 (1998).
14. Yakimov B.P., Davydov D.A., Fadeev V.V., Budylin G.S., Shirshin E.A. *Quantum Electron.*, **50** (1), 41 (2020) [*Kvantovaya Elektron.*, **50** (1), 41 (2020)].
15. Behm P., Hashemi M., Hoppe S., Wessel S., Hagens R., Jaspers S., Wenck H., Rubhausen M. *AIP Advances*, **7** (11), 115004 (2017).
16. Attas M., Posthumus T., Schattka B., Sowa M., Mantsch H., Zhang S.L. *Vibr. Spectrosc.*, **28** (1), 37 (2002).
17. van Logtestijn M.D., Dominguez-Huttinger E., Stamatas G.N., Tanaka R.J. *PLOS One*, **10** (2), e0117292 (2015).
18. Choe C., Lademann J., Darvin M.E. *Analyst*, **141** (22), 6329 (2016).
19. Verdier-Sevrain S., Bonte F. *J. Cosmet. Dermatol.*, **6** (2), 75 (2007).
20. Asogwa C.O., Lai D.T.H. *Electronics*, **6** (4), 82 (2017).
21. Xiao P., Wong W., Cottenden A.M., Imhof R.E. *Int. J. Cosmet. Sci.*, **34** (4), 328 (2012).
22. Wang J., Stantchev R.I., Sun Q., Chiu T.W., Ahuja A.T., MacPherson E.P. *Biomed. Opt. Express*, **9** (12), 6467 (2018).
23. Yang X., Zhao X., Yang K., Liu Y.P., Liu Y., Fu W.L., Luo Y. *Trends Biotechnol.*, **34** (10), 810 (2016).
24. Kekkonen E.A., Konovko A.A., Lee E.S., Lee I.M., Ozheredov I.A., Park K.H., Safonova T.N., Sikach E.I., Shkurinov A.P. *Quantum Electron.*, **50** (1), 61 (2020) [*Kvantovaya Elektron.*, **50** (1), 61 (2020)].
25. Alanen E., Nuutinen J., Nicklen K., Lahtinen T., Monkkonen J. *Skin Res. Technol.*, **10** (1), 32 (2004).
26. Clarys P., Clijsen R., Taeymans J., Barel A.O. *Skin Res. Technol.*, **18** (3), 316 (2012).
27. Bashkatov A.N., Genina E.A., Kochubey V.I., Tuchin V.V. *J. Phys. D: Appl. Phys.*, **38** (15), 2543 (2005).
28. Schleusener J., Lademann J., Darvin M.E. *J. Biomed. Opt.*, **22** (9), 91503 (2017).
29. Bertie J.E., Lan Z.D. *Appl. Spectrosc.*, **50** (8), 1047 (1996).
30. Bernatskiy A.V., Lagunov V.V., Ochkin V.N. *Quantum Electron.*, **49** (2), 157 (2019) [*Kvantovaya Elektron.*, **49** (2), 157 (2019)].
31. Nakagawa N., Matsumoto M., Sakai S. *Skin Res. Technol.*, **16** (2), 137 (2010).
32. Sdobnov A.Y., Tuchin V.V., Lademann J., Darvin M.E. *J. Phys. D: Appl. Phys.*, **50**, 285401 (2017).
33. Sdobnov A.Y., Darvin M.E., Schleusener J., Lademann J., Tuchin V.V. *J. Biophoton.*, **12** (5), e201800283 (2019).
34. Caspers P.J., Lucassen G.W., Carter E.A., Bruining H.A., Puppels G.J. *J. Investig. Dermatol.*, **116** (3), 434 (2001).
35. Crowther J.M., Sieg A., Blenkiron P., Marcott C., Matts P.J., Kaczvinsky J.R., Rawlings A.V. *Br. J. Dermatol.*, **159** (3), 567 (2008).
36. Choe C., Schleusener J., Choe S., Lademann J., Darvin M.E. *J. Biophoton.*, **13** (1), e201960106 (2020).
37. Choe C., Schleusener J., Choe S., Ri J., Lademann J., Darvin M.E. *Int. J. Cosmet. Sci.*, **42**, 482 (2020).
38. Choe C., Choe S., Schleusener J., Lademann J., Darvin M.E. *J. Raman Spectrosc.*, **50** (7), 945 (2019).
39. Sun Q. *Vibr. Spectrosc.*, **51** (2), 213 (2009).
40. Sun Q. *Chem. Phys. Lett.*, **568**, 90 (2013).
41. Gniadecka M., Nielsen O.F., Christensen D.H., Wulf H.C. *J. Investig. Dermatol.*, **110** (4), 393 (1998).
42. Kammeyer A., Luiten R.M. *Ageing Res. Rev.*, **21**, 16 (2015).
43. Gniadecka M., Nielsen O.F., Wessel S., Heidenheim M., Christensen D.H., Wulf H.C. *J. Investig. Dermatol.*, **111** (6), 1129 (1998).
44. Choe C., Schleusener J., Lademann J., Darvin M.E. *Mech. Ageing Dev.*, **172**, 6 (2018).
45. Boireau-Adamezyk E., Baillet-Guffroy A., Stamatas G.N. *Skin Res. Technol.*, **20** (4), 409 (2014).
46. Kottner J., Lichterfeld A., Blume-Peytavi U. *Arch. Dermatol. Res.*, **305** (4), 315 (2013).
47. Blume-Peytavi U., Kottner J., Sterry W., Hodin M.W., Griffiths T.W., Watson R.E., Hay R.J., Griffiths C.E. *Gerontologist*, **56** (2), S230 (2016).